An Oxygen-Rich Pyrochlore with Fluorite Composition

James B. Thomson, A. Robert Armstrong, and Peter G. Bruce[1]

School of Chemistry, University of St. Andrews, Purdie Building, St. Andrews, Fife KY16 9ST, United Kingdom

Oxygen has been intercalated into the pyrochlore $Ce_2Zr_2O_7$ by heating under oxygen at a moderate temperature. A composition approaching fluorite ($Ce_2Zr_2O_{7.97}$) has been obtained while retaining pyrochlore cation ordering. Whereas in fluorite all oxide ions are in tetrahedral sites, the oxygen-rich pyrochlore exhibits vacancies in some tetrahedral sites and occupancy of a new trigonal site. The latter arises from oxide ions in octahedral $32e$ sites within the pyrochlore cation array. © **1999 Academic Press**

INTRODUCTION

One of the most important targets for solid-state chemistry in the next century will be the controlled synthesis of given structures, something that is now commonplace in organic synthesis. The established techniques of solid-state chemistry do not lend themselves to such controlled syntheses. Intercalation chemistry offers one approach to target synthesis, since atoms can be inserted or extracted in a controlled manner, leading to new and predictable structures (1). In addition, these new compounds may be metastable unlike those prepared by conventional techniques and as a result they often exhibit unusual but desirable electrical, magnetic, and optical properties (2, 3). Intercalation may be chemical or electrochemical, the latter allowing much more precise tuning of the composition, and hence properties, of the intercalate than is possible by chemical synthesis as a result of the ability to control precisely the number of electrons flowing in an electric circuit. Intercalation plays an important role in the area of microporous solids with respect to their catalytic properties. Of no less importance is the essential part that lithium intercalation reactions play in the operation of electrodes for rechargeable lithium batteries. The development of such electrodes has been crucial in realizing this revolutionary technology over the last few years (4).

The study of intercalation extends beyond lithium as the guest to encompass other monovalent and divalent cations, as well as a range of molecular species (2, 5–10). In marked contrast the investigation of anion intercalation has received much less attention. The lack of studies aimed at a better understanding of oxygen intercalation in particular is surprising given the importance of oxide chemistry in general (11–15). The opportunity to modify oxides by the insertion or removal of oxygen in a controlled and predictable manner has much to offer the solid-state chemist and materials scientist alike. One need only think of the critical role played by oxygen stoichiometry in high-temperature superconductors to see the potential importance of oxygen intercalation. In the field of energy-related materials, solid oxide fuel cells require electrodes that are mixed electronic and oxide ion conductors; here again oxygen intercalation is important.

Pyrochlore oxides possess the general formula $A_2B_2O_7$. Their structure may be described as an ordered cubic close-packed array of cations with the oxide ions occupying seven-eighths of the tetrahedral sites between the cations. The pyrochlore structure is related to that of fluorite, AO_2, but with ordered cations and ordered vacancies in one-eighth of the tetrahedral anion sites. Pyrochlore oxides can exhibit a range of important and interesting behavior. The electrical properties of the pyrochlores can vary from insulating through semiconducting to metallic, and the insulating pyrochlores can demonstrate piezoelectric and ferroelectric behavior. Pyrochlore oxides can also sustain significant oxide ion conductivity even when stoichiometric, e.g., $Gd_2Zr_2O_7$ (16), unlike most other oxide ion conductors for which solid solutions must be formed, such as the doped fluorites, e.g., $Zr_{1-x}Ca_xO_{2-x}$.

We have intercalated oxygen into the pyrochlore $Ce_2Zr_2O_7$ using a solution-based route at room temperature but could achieve only a maximum oxygen content corresponding to $Ce_2Zr_2O_{7.36}$ (17, 18). Here we report what is, as far as we are aware, the first synthesis of a compound with the fluorite composition, $Ce_2Zr_2O_{7.97}$, but retaining the cation ordering of the pyrochlore structure, by low-temperature thermal oxidation.

EXPERIMENTAL

The host pyrochlore, $Ce_2Zr_2O_7$, has been prepared previously by two different routes (19, 20). One involved the

[1]To whom correspondence should be addressed. Fax: 44 1334 463808. E-mail: p.g.bruce@st-and.ac.uk.

rapid heating and combustion of aqueous solutions of cerium(III) nitrate and zirconium(IV) nitrate with carbohydrazide/urea in the required molar ratio; the second relied on the fusion of appropriate quantities of $BaCl_2$, $CeCl_3$, and $BaZrO_3$ under vacuum at $1000°C$ with subsequent leaching of $BaCl_2$. We have devised a simpler method. $Zr(OC_2H_5)_4$ (Aldrich, 98%) and $Ce_2(C_2O_4)_3$ (Aldrich, 99.9%) in appropriate molar ratios were added to 250 ml of distilled water; the mixture was placed in an ultrasonic bath for 2 h followed by vigorous stirring for 48 h. Approximately 200 ml of water was removed by rotary evaporation, with the remaining water being taken off by freeze-drying. The resulting powder was placed in an alumina crucible with a lid and transferred to a tube furnace. The sample was heated at $2°$/min to $250°C$ under an atmosphere of 95% Ar/5% H_2, this temperature being maintained for 30 min to permit decomposition of the organic material. The temperature was then raised at $10°$/min to $1300°C$ where it was held for 18 h and then cooled to room temperature again at $10°$/min. The samples were stored in an argon-filled glove box. To prepare the $Ce_2Zr_2O_{7.97}$ intercalate, $Ce_2Zr_2O_7$ was placed in an alumina boat in a tube furnace under flowing oxygen and then heated to $500°C$ for 22 h followed by slow cooling for 22 h while maintaining the oxygen flow. The host material is gray; however, the $Ce_2Zr_2O_{7.97}$ is pale yellowish orange.

Powder X-ray diffraction was carried out by sealing the samples in Lindemann tubes, which were then mounted on a Stoe STADI/P powder diffractometer operating in transmission mode and with $CuK\alpha_1$ radiation. Data were collected over the range $5° < 2\theta < 85°$ in steps of $0.02°$. Additional measurements were made on a Philips X-Pert system operating with Bragg–Brentano geometry and $CuK\alpha$ radiation.

Time-of-flight powder neutron diffraction data were collected at 298 K on the Polaris high-intensity, medium-resolution diffractometer at ISIS, Rutherford Appleton Laboratory [21]. Data from the highest-resolution backscattering detectors were refined by the Rietveld method using the CCSL suite of programs [22, 23]. Neutron scattering lengths used were $Zr = 0.7160$, $Ce = 0.4840$, and $O = 0.5803 \times 10^{-12}$ cm [24].

RESULTS AND DISCUSSION

The powder X-ray diffraction pattern of $Ce_2Zr_2O_{7.97}$, prepared as described above, consists of reflections that could be indexed on a cubic unit cell with the pyrochlore space group $Fd\bar{3}m$ (Fig. 1). Comparison with simulations confirms that the pyrochlore ordering is maintained (Figs. 1b, 1c). Examination of the powder neutron diffraction pattern (Fig. 2) for the intercalated compound indicated that whereas the majority of the reflections were consistent with the pyrochlore, $Fd\bar{3}m$, space group a significant number in the range 2.1 to 2.6 Å could not be attributed to this space

group or any known impurities. The Ce and Zr cations dominate the X-ray scattering, which means that this technique yields little information concerning the oxygen distribution; we may conclude only that the cation sublattice is very similar to that in the pyrochlore structure. The origin of the extra reflections in the neutron data must lie in the distribution of oxygen over the anion sublattice. These extra reflections could be accomodated either by reducing the symmetry to a primitive space group ($Pm\bar{3}m$) or by a doubling the unit cell. However, neither of these options permits retention of the cation ordering of the pyrochlore structure evident in the X-ray data, and so another model was sought. The only maximal nonisomorphic subgroup of $Fd\bar{3}m$ that permits the retention of Ce/Zr order is the cubic group $F1\bar{3}2/m$. The standard setting for this group is $R\bar{3}m$; hence we used this as the most appropriate means of describing the oxygen distribution for the purpose of executing the structure refinement. This does not imply that the lattice deviates metrically from cubic symmetry. Description of the pyrochlore structure in $Fd\bar{3}m$ may be translated into the lower-symmetry $R\bar{3}m$ subgroup. Table 1 lists the relevant crystallographic positions with their Wyckoff labels corresponding to each group. In the stoichiometric pyrochlore $Ce_2Zr_2O_7$ the oxide ions fully occupy two sets of tetrahedral sites labeled $48f$ and $8a$.

Rietveld refinement, using the neutron data, considered the possible occupancy of all the sites associated with the $R\bar{3}m$ space group listed in Table 1. Initial refinements indicated that the cation sites and the oxygen sites, O5–O10 (corresponding to the $48f$ sites in $Fd\bar{3}m$), are fully occupied to within e.s.d.s; as a consequence, the occupancy of these sites was fixed at unity in all subsequent refinements. The occupancy of the O1 to O4 sites in $R\bar{3}m$, which correspond to the $8a$ and $8b$ sites in $Fd\bar{3}m$, refined to 1.00(5), 0.77(4), 0.81(9), and 0.74(3), respectively. The total occupancy of O1–O10 sites corresponds to a stoichiometry of $Ce_2Zr_2O_{7.59(7)}$. In addition to the tetrahedrally coordinated anion sites $48f$, $8a$, and $8b$ in $Fd\bar{3}m$, there is also an octahedral site at the $32e$ position ($\frac{1}{4}$, $\frac{1}{4}$, $\frac{1}{4}$). This splits into five octahedral sites in $R\bar{3}m$ but exploration of these positions by profile refinement indicated occupancy of only the O11 site (Table 1). Subsequent difference Fourier maps encompassing the entire asymmetric unit revealed no evidence of significant remaining scattering density. In the final refinement the occupancies of the O1 to O4 and O11 sites were allowed to vary independently and yielded a composition for the oxide of $Ce_2Zr_2O_{7.97(12)}$. The introduction of the O11 site led to an improvement in χ^2 of 22%.

Examination of the refined atomic coordinates (Table 2) confirms the result from X-ray diffraction that there is little change in the cation sublattice, with deviation from the ideal pyrochlore structure being confined largely to the anion sublattice. This coupled with the fact that the cell remains metrically cubic to within 1 e.s.d [$\alpha = 90.05(6)°$] means that
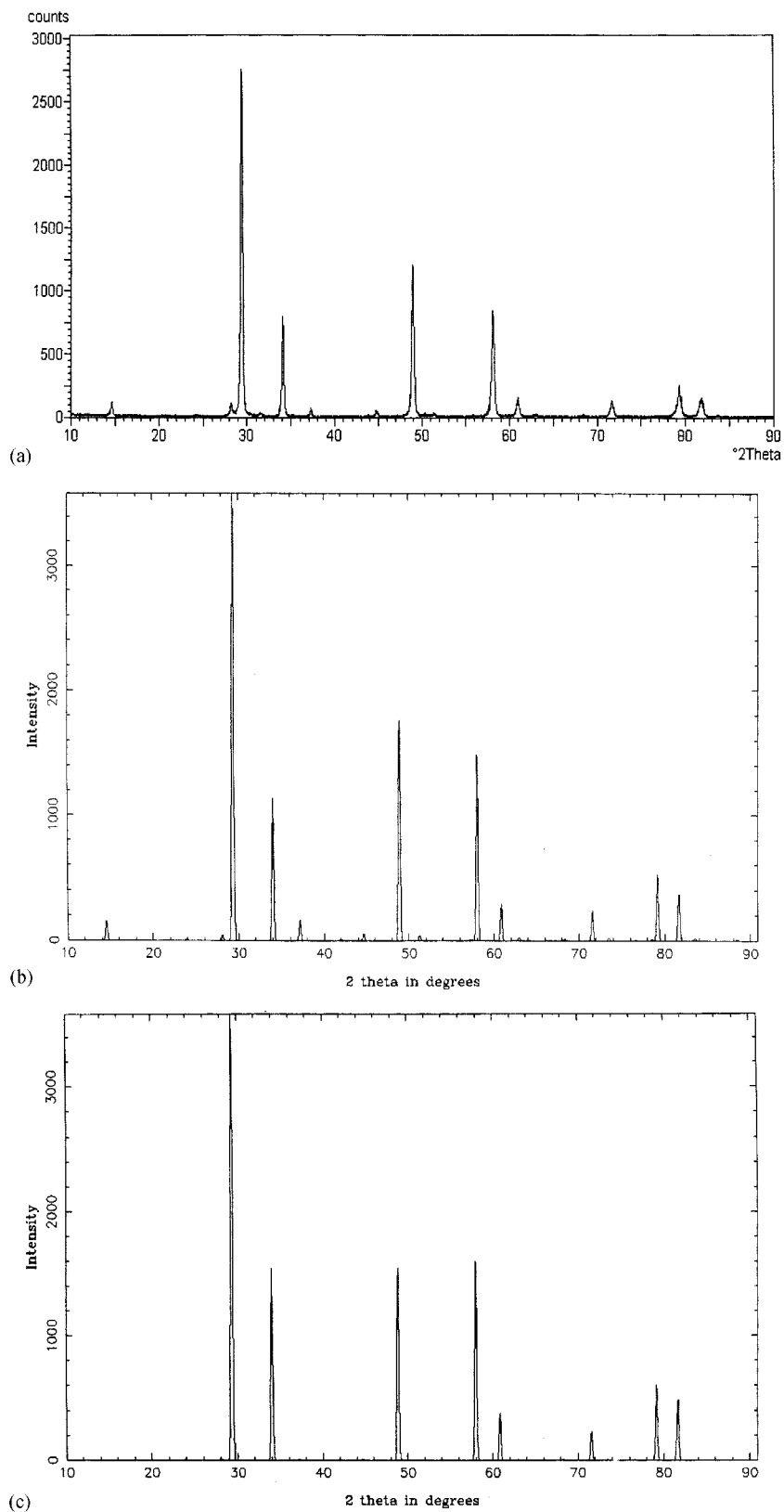
FIG. 1. (a) Powder X-ray diffraction pattern for $Ce_2Zr_2O_{7.97}$. A small quantity of tetragonal zirconia is present as an impurity. (b) Simulated diffraction pattern for pyrochlore $Ce_2Zr_2O_7$. (c) Simulated diffraction pattern for pyrochlore $Ce_2Zr_2O_7$ with disordered Ce/Zr (i.e., the cation arrangement in fluorite).

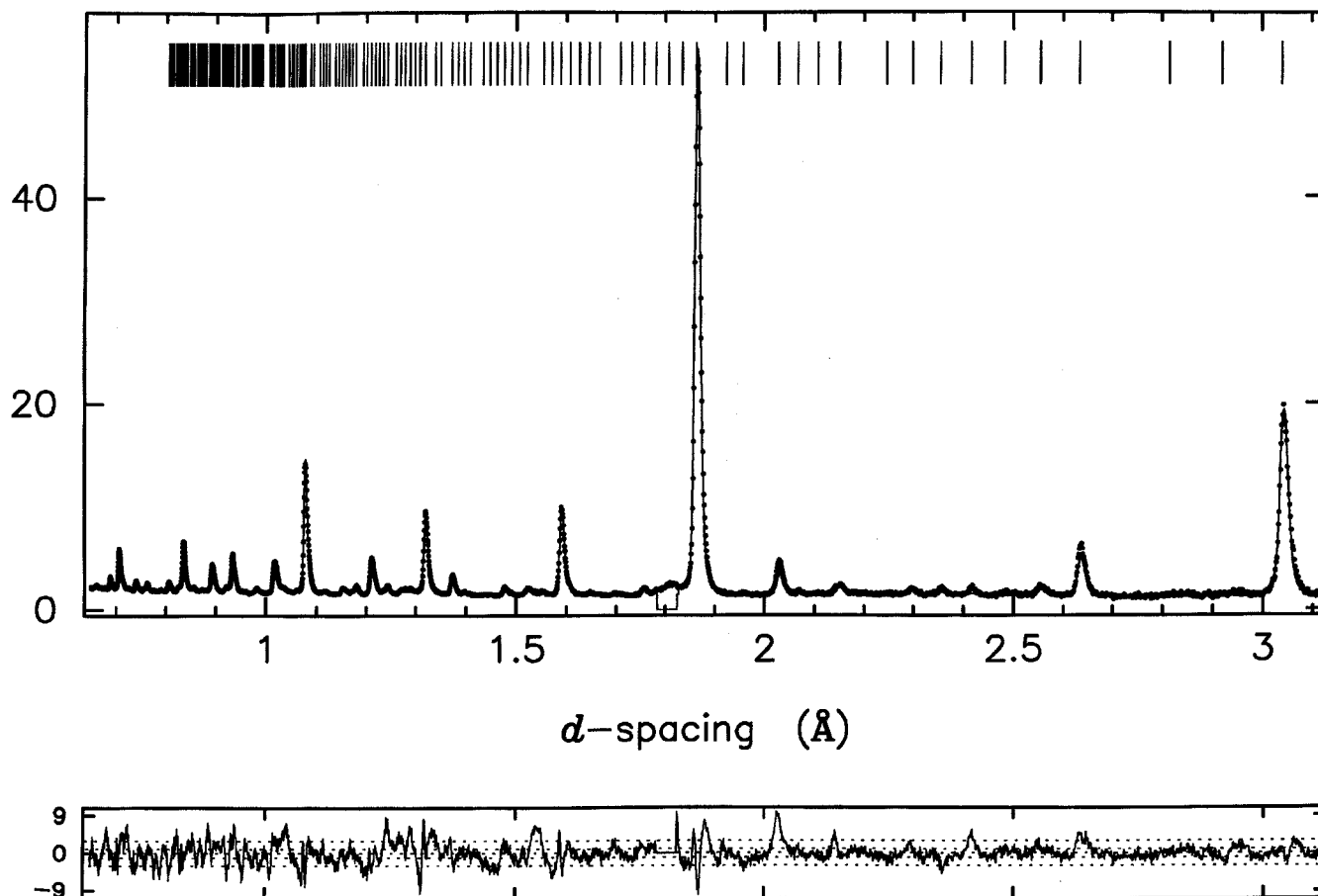**FIG. 2.** Neutron profile fit for $Ce_2Zr_2O_{7.97}$. Experimental data shown as dots, profile fit as a continuous line, and difference/e.s.d. at the bottom.

for the purpose of understanding the crystal chemistry and relating it to the host $Ce_2Zr_2O_7$, it is helpful to describe the structure of $Ce_2Zr_2O_{7.97}$ by referring to the cubic pyrochlore. The structure of $Ce_2Zr_2O_{7.97}$ consists of cubic close-packed cations ordered in the usual pyrochlore arrangement. A view of the structure emphasizing the oxygen coordination around the different cation sites is shown in Fig. 3a. Those coordination polyhedra that are somewhat obscured in Fig. 3a are shown individually in Fig. 3b. The tetrahedrally coordinated anion sites at the 48*f* positions in $Fd\overline{3}m$ (O5 through O10 in $R\overline{3}m$) are fully occupied, whereas the remaining 8*a* and 8*b* tetrahedral sites ($Fd\overline{3}m$), corresponding respectively to the O1/O2 and O3/O4 sites in $R\overline{3}m$, are partially occupied. The coordination environments around the oxygens are shown in Fig. 4a. The sum of the occupancies of O1 and O2, expressed in terms of the 8*a* sites ($Fd\overline{3}m$), is 0.79(2), whereas that for O3 and O4 corresponds to 0.53(7). It is interesting that insertion of additional oxygen does not continue to fill the 8*a* or 8*b* sites but involves population of a new site. We may speculate that the abrupt increase in energy associated with the apparent need to occupy a new site when the oxygen composition exceeds

7.36, despite vacancies in 8*a* and 8*b*, is related to this value being the limit of oxygen insertion at room temperature, $Ce_2Zr_2O_{7.36}$ (17, 18). The O11 site is surrounded by 3Zr(Zr2, Zr3, Zr4) and 3Ce(Ce2, Ce3, Ce4) ions. The Zr4–O11 bond length is 3.26(4) Å (Table 3), which is too long to be considered as a bond; thus at first sight the oxygen appears to exist in a square-pyramidal environment composed of Ce2, Ce3, Ce4, Zr2, and Zr3. However, the shortest Zr–O11 distance is 2.88Å compared with the average Ce–O11 distance of 2.24 Å. Therefore the oxygen in the O11 site is best regarded as existing in a 3-coordinate environment formed by the three Ce ions, one face of the octahedron; i.e., it is in a trigonal site (Fig. 4d). The oxygen ions coordinating Zr are located in the O3 to O10 sites and the combined oxygen content of these sites yields an average coordination number around zirconium of 7. This is known to be a preferred cordination for Zr in an oxygen environment; for example, it is found in the room-temperature structure of ZrO_2. It is probable that the preference for a 7-coordinate zirconium ion determines the O3/O4 occupancy. Although Ce1 is coordinated by 2 × O1 and 6 × O10 sites which are both fully occupied resulting in an 8

TABLE 1
Atomic Coordinates for the $Ce_2Zr_2O_{7.97}$ Model in Space Group $R\bar{3}m$ with Equivalent Site $Fd\bar{3}m$ Symbols[a]

Atom	Site	x	y	z	$Fd\bar{3}m$ site
Ce1	1a	0	0	0	Ce, 16c
Ce2	3e	0	$\frac{1}{2}$	$\frac{1}{2}$	Ce, 16c
Ce3	6h	0.2500	0.2500	0.000	Ce, 16c
Ce4	6g	0.2500	− 0.2500	$\frac{1}{2}$	Ce, 16c
Zr1	1b	$\frac{1}{2}$	$\frac{1}{2}$	$\frac{1}{2}$	Zr, 16d
Zr2	3d	$\frac{1}{2}$	0	0	Zr, 16d
Zr3	6f	0.2500	− 0.2500	0.0000	Zr, 16d
Zr4	6h	0.2500	0.2500	0.5000	Zr, 16d
O1	2c	0.1250	0.1250	0.1250	O2, 8a
O2	6h	0.3750	0.3750	0.1250	O2, 8a
O3	2c	0.3750	0.3750	0.3750	O3, 8b
O4	6h	0.8750	0.8750	0.3750	O3, 8b
O5	6h	0.39	0.1250	0.1250	O1, 48f
O6	12i	0.36	0.1250	0.6250	O1, 48f
O7	12i	0.11	0.8750	0.3750	O1, 48f
O8	6h	0.16	0.3750	0.3750	O1, 48f
O9	6h	0.37	0.6250	0.6250	O1, 48f
O10	6h	0.85	0.1250	0.1250	O1, 48f
O11	12i	0.0000	0.5000	0.7500	O, 32e

[a] Fractions indicate special positions.

coordinate site, Ce2, Ce3, and Ce4 are coordinated by eight tetrahedral sites and the O11 site. In the case of Ce2 and Ce3 there are $4 \times$ O11 sites immediately coordinating these ions, whereas there are only 2 in the case of Ce4. As a result Ce2, Ce3, and Ce4 have average coordination numbers that exceed 8 and are respectively 9.2, 8.6, and 8.3. The average

TABLE 2
Refined Structural Data for $Ce_2Zr_2O_{7.97}$[a]

Atom	Site	x	y	z	B_{iso} (Å^2)	Occup.
Ce1	1a	0.0	0.0	0.0	− 0.04(11)	
Ce2	3e	0.0	$\frac{1}{2}$	$\frac{1}{2}$	− 0.04(11)	
Ce3	6h	0.2404(13)	0.2404(13)	− 0.005(2)	− 0.04(11)	
Ce4	6g	0.2581(13)	− 0.2581(13)	$\frac{1}{2}$	− 0.04(11)	
Zr1	1b	$\frac{1}{2}$	$\frac{1}{2}$	$\frac{1}{2}$	0.50(6)	
Zr2	3d	$\frac{1}{2}$	0.0	0.0	0.50(6)	
Zr3	6f	0.2505(12)	− 0.2505(12)	0.0	0.50(6)	
Zr4	6h	0.2467(11)	0.2467(11)	0.495(2)	0.50(6)	
O1	2c	0.119(2)	0.119(2)	0.119(2)	0.33(3)	1.00(5)
O2	6h	0.387(2)	0.387(2)	0.108(2)	0.33(3)	0.72(3)
O3	2c	0.379(5)	0.379(5)	0.379(5)	0.33(3)	0.38(13)
O4	6h	0.890(2)	0.890(2)	0.380(3)	0.33(3)	0.58(5)
O5	6h	0.387(2)	0.125(2)	0.125(2)	0.33(3)	
O6	12i	0.3619(11)	0.1209(13)	0.6209(15)	0.33(3)	
O7	12i	0.1126(10)	0.8728(15)	0.3740(13)	0.33(3)	
O8	6h	0.1650(14)	0.3672(12)	0.3672(12)	0.33(3)	
O9	6h	0.368(2)	0.619(2)	0.619(2)	0.33(3)	
O10	6h	0.8503(15)	0.1276(14)	0.1276(14)	0.33(3)	
O11	12i	0.0615(12)	0.511(2)	0.734(2)	0.33(3)	0.44(2)

[a] Space group $R\bar{3}m$, $a = 10.5439(2)$ Å, $\alpha = 90.05(6)°$, $\chi^2 = 9.58$, $R_{wp} = 5.35\%$, 3048 observations, 52 variables, 1374 reflections.

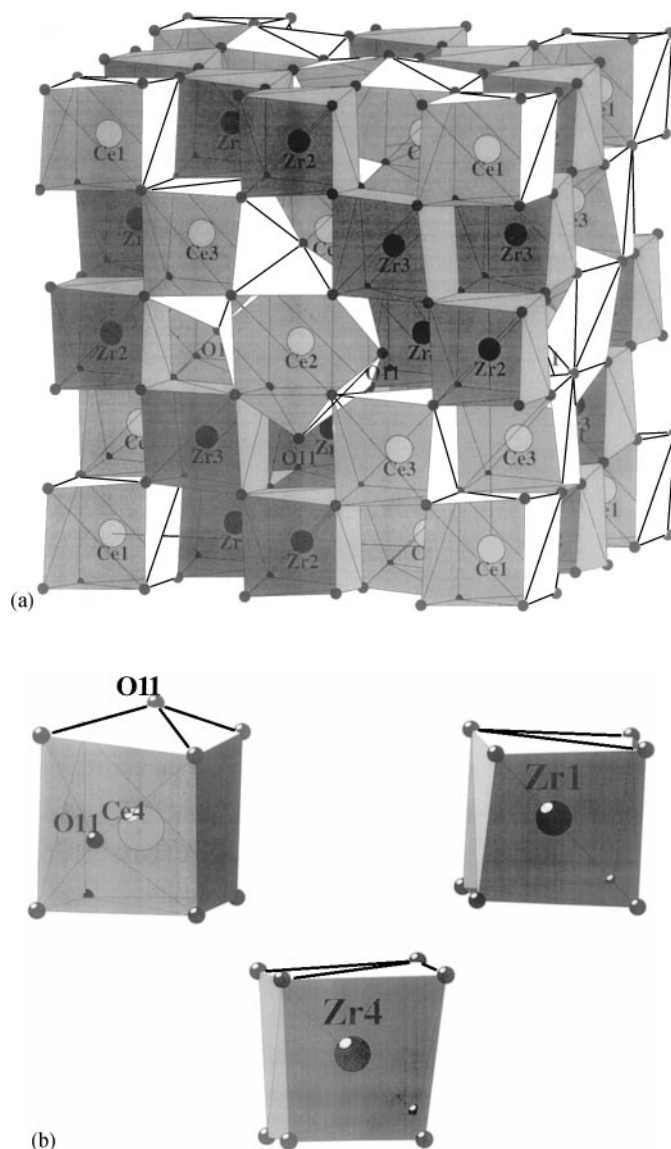**FIG. 3.** (a) Structure of $Ce_2Zr_2O_{7.97}$ showing cation coordination environments. (b) Coordination polyhedra for Ce4, Zr1, and Zr4 in $Ce_2Zr_2O_{7.97}$.

coordination number for all four Ce ions in this structure is 8.4.

Occupancy of the O11 sites introduces some short O–O distances. Intercalation reactions often lead to high-energy, metastable compounds, and as shown below the oxygen-rich pyrochlore $Ce_2Zr_2O_{7.97}$ is no exception. As we have shown previously, the O11 site is not occupied by oxygen intercalation under mild conditions at room temperature (18), it is only involved after more stable sites have been occupied. We cannot rule out the presence of peroxide linkages, although the pale yellow color of the compound and the magnetic data presented below suggest a fully oxidized cation array.
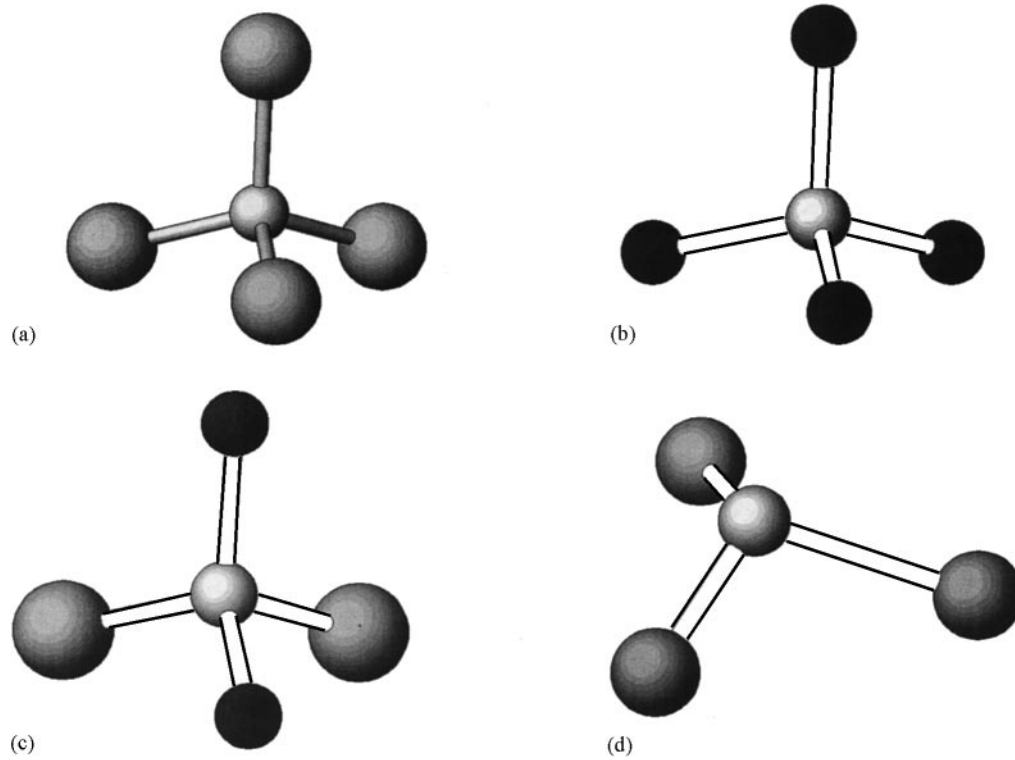
FIG. 4. Coordination environments for oxygen in $Ce_2Zr_2O_{7.97}$. (a) O1 ($8a$ site in $Fd\overline{3}m$)—$3 \times Ce3 + 1 \times Ce1$. (b) O3 ($8b$ site in $Fd\overline{3}m$)—$3 \times Zr4 + 1 \times Zr1$. (c) O10 ($48f$ site in $Fd\overline{3}m$)—$2 \times Zr3 + 1 \times Ce1 + 1 \times Ce3$. Ce, large pale circles; Zr, small dark circles. (d) Trigonal coordination environment of O11 ($1 \times Ce2$, $1 \times Ce3$, $1 \times Ce4$).

To verify that the composition is close to $Ce_2Zr_2O_8$, magnetic measurements were carried out at the University of Edinburgh. A sample of the oxide was placed in a Squid magnetometer (Model MPMS2, Quantum Design) and, assuming values for g and J of $\frac{6}{7}$ and $\frac{5}{2}$ respectively, for Ce^{3+}, the data indicate that no more than 5% of the cerium is in the trivalent state; i.e., the composition as determined by this method is between $Ce_2Zr_2O_{7.95}$ and $Ce_2Zr_2O_8$. This verifies that the pale yellowish-orange solid formed after oxidation at $500°C$ does closely approximate the fluorite composition.

Since $Ce_{1-x}Zr_xO_2$ solid solutions with the fluorite structure are known to form by high-temperature solid-state reaction, it is likely that the pyrochlore $Ce_2Zr_2O_{7.97}$ is metastable. To examine this a combined TGA/DTA study was carried out in 1 atm of flowing oxygen up to $900°C$. A small thermal event was observed in the DTA at $700°C$. Subsequent powder X-ray diffraction indicated a reduction in the relative intensities of the peaks associated with the cation ordering. Evidently the cations of the pyrochlore structure slowly disorder, eventually forming the more stable fluorite structure.

TABLE 3
Selected Bond Distances for $Ce_2Zr_2O_{7.97}$ Sample

Bond	Distance (Å)	Bond	Distance (Å)
Ce1–O1 × 2	2.17(2)	Ce1–O10 × 6	2.47(3)
Ce2–O2 × 2	2.03(3)	Ce2–O6 × 4	2.32(2)
Ce2–O8 × 2	2.64(2)	Ce2–O11 × 4	2.55(3)
Ce3–O1	2.23(4)	Ce3–O2	2.44(5)
Ce3–O5 × 2	2.40(4)	Ce3–O7 × 2	2.34(4)
Ce3–O8	2.60(4)	Ce3–O10	2.27(4)
Ce3–O11 × 2	2.70(4)		
Ce4–O2 × 2	2.40(4)	Ce4–O6 × 2	2.41(3)
Ce4–O7 × 2	2.45(3)	Ce4–O9 × 2	2.14(4)
Ce4–O11 × 2	2.08(4)		
Zr1–O3 × 2	2.21(9)	Zr1–O9 × 6	2.26(3)
Zr2–O4 × 2	2.07(4)	Zr2–O5 × 2	2.21(3)
Zr2–O7 × 4	2.23(2)	Zr2–O11 × 4	2.88(3)
Zr3–O4 × 2	2.32(4)	Zr3–O6 × 2	2.20(3)
Zr3–O7 × 2	2.19(3)	Zr3–O10 × 2	2.15(3)
Zr3–O11 × 2	2.82(3)		
Zr4–O3	2.32(9)	Zr4–O4	2.43(5)
Zr4–O5	2.14(4)	Zr4–O6 × 2	2.24(3)
Zr4–O8 × 2	2.04(3)	Zr4–O9	2.47(4)
Zr4–O11	3.26(4)		

REFERENCES

1. C. N. R. Rao, "Chemical Approaches to the Synthesis of Inorganic Materials." Wiley, New York, 1994.

2. D. O'Hare, *in* "Inorganic Materials" (D. W. Bruce and D. O'Hare, Eds.), Wiley, New York, 1992.

3. A. J. Jacobson and M. S. Whittingham (Eds.), "Intercalation Chemistry." Academic Press, San Diego, 1982.

4. P. G. Bruce, *Philos. Trans. R. Soc. London A* **354,** 1577 (1996).

5. P. G. Bruce, J. Nowinski, V. C. Gibson, Z. V. Hauptman, and A. Shaw, *J. Solid State Chem.* **89,** 202 (1990).

6. I. Abrahams, J. L. Nowinski, P. G. Bruce, and V. C. Gibson, *J. Solid State Chem.* **94,** 254 (1991).

7. P. G. Bruce, F. Krok, J. Nowinski, V. C. Gibson, and K. Tavakkoli, *J. Mater. Chem.* **1,** 705 (1991).

8. P. G. Bruce, F. Krok, P. Lightfoot, and J. L. Nowinski, *Solid State Ionics* **53–56,** 351 (1992).

9. P. G. Dickens, A. M. Chippindale, and S. J. Hibble, *Solid State Ionics* **34,** 79 (1989).

10. P. G. Dickens, S. V. Hawke, and M. T. Weller, *Mater. Res. Bull.* **19,** 543 (1984).

11. J-C. Grenier, A. Wattiaux, J-P. Doumerc, P. Dordor, L. Fournes, J-P. Chaminade, and M. Pouchard, *J. Solid State Chem.* **96,** 20 (1992).

12. A. Wattiaux, J. C. Park, J-C. Grenier, and M. Pouchard, *C. R. Acad. Sci. Paris* **310,** 1047 (1990).

13. P. Rudolf and R. Schöllhorn, *J. Chem. Soc. Chem. Commun.*, 1158 (1992).

14. S. Bhavaraju, J. F. Di Carlo, D. P. Scarfe, A. J. Jacobson, and D. J. Buttrey, *Solid State Ionics* **86–88,** 825 (1996).

15. P. G. Radaelli, J. D. Jorgensen, A. J. Schultz, B. A. Hunter, J. L. Wagner, F. C. Chou, and D. C. Johnston, *Phys. Rev. B* **48,** 499 (1993).

16. H. L. Tuller, S. Kramer, and M. A. Spears, *in* "High Temperature Electrochemistry." 14th Riso Symposium, Denmark, 1993, p. 151.

17. J. B. Thomson, A. R. Armstrong, and P. G. Bruce, *J. Chem. Soc. Chem. Commun.*, 1165 (1996).

18. J. B. Thomson, A. R. Armstrong, and P. G. Bruce, *J. Am. Chem. Soc.* **118,** 11129 (1996).

19. J. J. Casey, L. Katz, and W. C. Orr, *J. Am. Chem. Soc.* **77,** 2187 (1955).

20. N. A. Dhas and K. C. Patil, *J. Mater. Chem.* **3,** 1289 (1993).

21. R. I. Smith, S. Hull, and A. R. Armstrong, *Mater. Sci. Forum* **166–169,** 251 (1994).

22. J. C. Matthewman, P. Thompson, and P. J. Brown, *J. Appl. Crystallogr.* **15,** 167 (1982).

23. P. J. Brown and J. C. Matthewman, Rutherford Appleton Laboratory Report, RAL-87-010 (1987).

24. V. F. Sears, *Neutron News* **3**(3), 26 (1992).